Rainfall regionalization and variability of extreme precipitation using artificial neural networks: a case study from western central Morocco

Abdelhafid El Alaoui El Fels, Mohamed El Mehdi Saidi, Assma Bouiji and Mounia Benrhanem

ABSTRACT

Here, we investigate the precipitation regionalization and the spatial variability of rainfall extremes, using a 47-year long station-based dataset from western central Morocco, a region with marked topographic and climatic variations. The principal component analysis revealed three homogeneous rainfall regimes, consistent with topographic features: the coastal area receives heavy rainfall during autumns and winters, whereas the inner lowlands, in the middle of the study area, are characterized by an overall rainfall deficit regardless of their high water demand for irrigation, and the highest rainfall amounts take place in the mid-mountain area, including the summer seasons. Furthermore, the frequency analysis of daily rainfall extremes revealed high ten-year precipitation amounts in the coastal region (about 88 mm) and exceptional daily precipitation for longer return periods (182 mm for a 100-year period). Using artificial neural networks, the spatialization of these extreme precipitation events shows that they increase from the plain to the Atlas mountains and especially from the plain to the Atlantic Ocean. The spatial distribution of extreme precipitation highlights the areas where stormwater management needs to be improved, such as efficient stormwater drainage, and where floods are more likely to take place in the future.

Key words | artificial neural networks, Morocco, precipitation extremes, principal components analysis, rainfall regionalization, rainfall variability

Abdelhafid El Alaoui El Fels (corresponding author)
Mohamed El Mehdi Saidi
Laboratory of Geo-Sciences and Environment,
Cadi Ayyad University,
Marrakech,
Morocco
E-mail: elalaoui.abdelhafid@gmail.com

Assma Bouiji
Laboratory of Geodynamic, Geomatic and Geotechnic,
Cadi Ayyad University,
Marrakech,
Morocco

Mounia Benrhanem
Hydraulic Basin Agency of Tensift,
Marrakech,
Morocco

INTRODUCTION

Water resources management for agricultural, industrial, or domestic use is closely linked to a thorough knowledge of climatic vectors, including precipitation (Hiez 1977) which is often disturbed by the variability of rainfall intensity. Indeed, the variability is a climatic feature that has become more influential than the long-term average (Whitford 2002). This is particularly the case in arid and semi-arid climate areas, where populations must adapt to the recurrent

dry periods which are often interrupted by short precipitation extreme events. Hence, the delineation of homogeneous rainfall areas is essential to understand regional climate regimes and to better manage the meteoric water resources.

In this context, rainfall regionalization has become necessary in semi-arid and arid environments (such as central and southern Morocco, respectively) for various purposes; in particular, agricultural planning, drought analysis, design of water management structures, and land use planning. Therefore, one of the most widely used methods for distinguishing different rainfall regimes is multivariate statistical analysis (Malmgren & Winter 1999; Härdle &

Simar2012). Principal component analysis (PCA), which is a very popular multivariate statistical analysis method (Son *et al.* 2017; Ding *et al.* 2019; Kim *et al.* 2018; Cai *et al.* 2019; Li *et al.* 2019), is an example that allows identifying homogeneous rainfall groups and grouping different sites that have similar characteristics (e.g., similar rainy seasons), as well as the delimitation of climatic regions with regards to their meteorological behavior. Frequency analysis of maximum rainfall is another method of fundamental interest for forecasting hydro-pluviometric extremes.

Furthermore, in recent decades, several researchers have proposed that precipitation extremes tend to be more intense and more frequent (New *et al.* 2001; Planton *et al.* 2005; Solomon *et al.* 2007). Distinguishing precipitation extremes is of great interest for differentiating regular annual cumulative rainfall (favorable for agriculture) and precipitation that occurs in the form of intense showers, which are separated by long dry sequences and are harmful to soils and agricultural yields. This is very alarming, considering that rainfall studies, for the inventory and management of water resources for example, have been focused on the trends of average rainfall amount without giving enough attention to the behavior of precipitation extremes. The lack of research into precipitation extremes often stems from not having access to short time step data (Goula *et al.* 2012), especially in developing countries.

In this study, we aim to analyze the frequency of daily rainfall extremes and their probability of occurrence in western central Morocco. It is an important agricultural region and water scarcity is expected to be one of the key water challenges. Using the PCA, a rainfall regionalization will be performed to distinguish homogeneous rainfall regions. Furthermore, using artificial neural networks (ANN), spatial variability of precipitation extremes will also be examined in order to provide a regional overview of the organization of these extremes.

MATERIAL AND METHODS

Study area and data

The Tensift basin is a watershed located in western central Morocco with the main tributary leading to the Atlantic Ocean. Tensift is located between the latitudes 30° 50′ and 32° 10′ north and the longitudes 7° 25′ and 9° 25′ west (Figure 1). The basin consists of a broad alluvial plain, that is generally arid, and a vigorous mountainous area in the south, which collects and transports most surface water to the plain. The mainstream flows from east to west with a total length of approximately 260 km. This temporary *wadi* (Arabic term for a valley, that is often dry, except during the rainy season) drains a catchment of 18,500 km², where altitudes range from 43 to 4,167 m.a.s.l. (meters above sea level) (the highest peak in North Africa). The slopes generally become stronger from the plain towards the High Atlas Mountains, with an average exceeding 20°. The most common orientations of the slopes are north, west, and north-west.

The Tensift catchment is exposed to the rainy disturbances originating from the Atlantic Ocean. However, the climate is characterized by relative aridity in the inner plain (less than 250 mm of rainfall per year). Acuteness of this aridity is conditioned by the low altitude and the sub-Saharan latitude. Contrariwise, the mountains are characterized by a heavy rainfall (more than 500 mm per year) and perennial fluvial flows. The seasonal contrast is very marked in the mountains and the rainy events are usually more frequent during autumn (Sep–Oct–Nov) and winter (Dec–Jan–Feb) (Saidi *et al.* 2012). These events are irregular, hard to predict, and sometimes intense and violent. During the rest of the year, drought mainly occurs in the lowland area where temperatures are high and evaporation rates are important. The annual thermal amplitude is also quite considerable, with temperatures reaching up to 45 °C during summers (Jun–Jul–Aug) and dropping to below 5 °C during winters.

The data used in this study consist of daily and monthly precipitation retrieved from 16 meteorological stations located over altitudes ranging from 53 to 1,100 meters (Figure 1, Table 1). These data cover a 47-year period (1970/71 to 2016/17).

Principal component analysis

PCA is a descriptive statistical analysis that releases as much information as possible from a data table, information like optimal graphic representation of individuals (lines) and variables, by best explaining the initial links between these
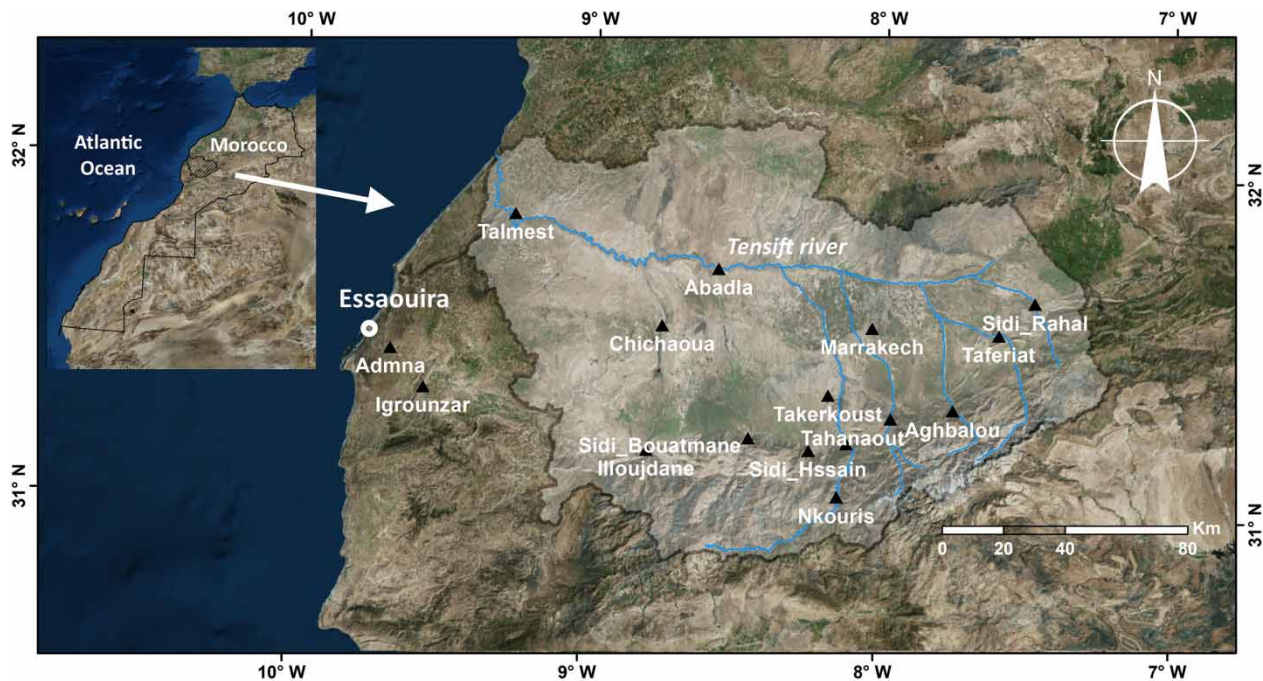
Figure 1 | Geographical location of Tensift catchment in western central Morocco, showing the locations of the meteorological stations where precipitation data were retrieved for this study.

Table 1 | List of the meteorological stations of Tensift watershed where data were retrieved for this study, showing the corresponding altitude and annual rainfall of each site

Stations	Altitude (m)	Mean annual rainfall (mm)
Abadla	250	171
Admna	70	327
Aghbalou	1,070	532
Chichaoua	340	182
Igrounzar	158	283
Illoujdane	757	314
Imin_El_Hammam	770	379
Marrakech	460	235
Nkouris	1,100	220
Sidi_Bouatmane	820	357
Sidi_Hssain	1,030	418
Sidi_Rahal	690	342
Taferiat	760	347
Tahanaout	925	370
Takerkoust	630	233
Talmest	53	280

variables (that are extreme precipitations) (Smith 1991; Ringnér 2008). In our case, this table consists of individuals (rainfall data from 16 stations) and variables (47 years of monthly rainfall amount). The first main component is that for which the variance of the observations is maximal and which better illustrates the dispersion of the observations. The other components are also classified according to the degree of their explanation of the variation of the observations.

Frequency analysis

For the frequency analysis, many statistical laws allow the statistical adjustment of extreme weather events, in order to assess how the chosen law reproduces the observed data. Different laws have been applied in different parts of the world. For example, the US Water Resources Board recommended Log Pearson 3 distribution (Benson 1968), while a similar study in the United Kingdom (NERC 1975) proposed the generalized extreme value (GEV) distribution. In Russia, it is the generalized

Gamma distribution that has been recommended (Kritsky & Menkel 1969), and the Log-logistic law is applied in China (Shao *et al.* 2004), while Pearson 3 and Log Pearson 3 distributions were generally recommended in Germany and Australia (IEA 1977). For maximum daily rainfall, although Gumbel and Weibul distributions (Papalexiou & Koutsoyiannis 2006) have long been the most used models for estimating quantiles, Rossi *et al.* (1984) found that the extreme value law, that has two parameters (scale and shape parameters) (TCEV: two-component extreme value) fitted as well. However, other researchers, more numerous, prefer the law of extreme values (GEV) and the Log-normal law to model a set of maximum daily rainfall (Wilks & Cember 1993; Chaouche *et al.* 2002; Koutsoyiannis 2004; Onibon *et al.* 2004), including applications in the neighboring countries of Morocco: Spain (Ferrer 1992), Algeria (Habibi *et al.* 2012) and Tunisia (Merzougui & Slimani 2012).

Additionally, several fitting probabilistic models are used in hydrology: the weighted moment method (WM) (Greenwood *et al.* 1979), the maximum likelihood (ML) method (Fisher 1922), and the L-moments method (LM) (Hosking 1990). Currently, the WM method is considered the most robust and the most effective method (Rao & Hamed 2000; Kidson & Richards 2005), generally used for hydrological data analysis (Wania *et al.* 2017; Raqab *et al.* 2018), as the estimation of its parameters has shown very good statistical properties for large samples. Therefore, we chose the WM method to adjust our models.

After adjusting the models, the numerical confirmation of graphical results is necessary for selecting the most suitable frequency models. This selection can be formalized as follows:

- A sample of size n $D = x1; \ldots ; xn$, is available in ascending order.
- The sample is taken from an unknown parent distribution f (x).
- M_j, $j = 1; \ldots ; N_m$ are the operating models used to represent the observed data.
- The observed data are in the form of probability distributions, $M_j = g_j(x; \widehat{\theta})$.
- (θ) are the parameters estimated from the available data sample D.

The purpose of the model selection is to identify the optimal model (M_{opt}) that is best suited to represent the data, i.e., the model closest to the parent distribution f (x).

However, the adoption of evaluation criteria for these laws is required to better evaluate their suitability for the analyzed samples, because, with many possible models, there would be different statistical combinations of explanatory variables. Two criteria of selection, the most used in the literature, will be taken into account, namely, the Akaike information criterion (AIC) (Akaike 1974) and the Bayesian information criterion (BIC) (Schwarz 1978). These criteria are given by the following equations:

Akaike's information criterion (Akaike 1974):

$$AIC = -2Ln(L) + 2K$$

where L is the maximized value of the likelihood function for the estimated model and K is the number of parameters in the estimated model.

For $ARMA(p, q)$ models $K = p + q$, and the AIC can be calculated as:

$$AIC(p, q) = Tlog(\sigma) + 2(p, q)$$

where σ is the variance of the innovation process.

Bayesian information criterion (Schwarz 1978):

$$BIC = -2Ln(L) + KLn(T)$$

where T is the number of observations. For $ARMA(p, q)$ models, $K = p + q$ and the BIC can be calculated as:

$$BIC(p, q) = Tlog(\sigma) + LnT(p, q)$$

This criterion therefore represents a compromise between bias (which decreases with the number of parameters) and parsimony (description of the data with the minimum of possible parameters) (Lancelot & Lesnoff 2005). A few years later, Schwarz (1978) developed BIC, derived from AIC. Unlike the latter, the penalty depends on the size of the sample and not just the number of parameters. Therefore, we will use these two criteria to choose the appropriate distribution.

Artificial neural networks (ANN)

The spatial distribution of an element is a classical problem of estimating a function $f(x)$, where $x = (x, \ y)$, at a point x_p of the plan from known values of f into a number m, of surrounding points x_i:

$$f(x_p) = \sum_{i=1}^{m} w_i * f(x_i)$$

The problem is to determine the weighting, w_i, of each of the surrounding points. There are many ways to choose these weights, including the two best-known methods: linear interpolation (based on the inverse distance weighting) and the cubic spline interpolation (adjustment of cubic polynomials). However, these approaches are limited by their inability to integrate the distance from the shore and the altitudinal effects. Therefore, here, we suggest a method of spatial distribution based on a neural networks approach: the multilayer network (McCulloch & Pitts 1943). Neural networks belong to the category of 'black box' models, which are mathematical tools of approximation inspired by the functioning of biological nervous systems. This modeling tool can typically be represented by three types of neuron layers: an input layer, one or more hidden layer(s), and an output layer. Each layer has a set of interconnected signal processing units, called artificial neurons. Each connection point (called coefficient or weight), between two neurons, plays the role of a synapse. The mathematical representation of the neuron introduced by McCulloch & Pitts (1943) is illustrated in Figure 2. Each cell receives inputs in a vector form (X), performs a weighted sum (α), and generates using a linear or non-linear transfer function (G), a real result (Y) of the form:

$$Y = G(W * X + b)$$

where $W = (w_{i,1}, w_{i,2}, \ldots, w_{i,N})$ is the matrix of neuron weights i, $X = (x_1, x_2, \ldots, x_N)$ are the inputs of the neuron i, b is the bias of the neuron, and $\alpha = (W * X + b)$ is the weighted sum of the inputs called net or potential inputs of the neuron i and constitutes the argument of the activation function G of the neuron i. The classical nonlinear
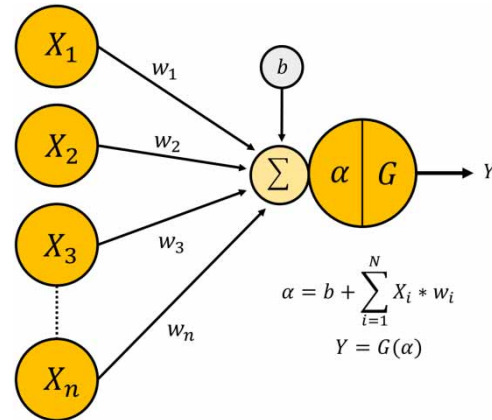

Figure 2 │ The artificial neuron structure, as described in artificial neural networks (McCulloch & Pitts 1943).

activation function is the sigmoid function inspired by the formal neuron of McCulloch & Pitts (1943), defined by:

$$G(\alpha) = (1 - \exp(-\alpha))^{-1}$$

The adjustment of ANN is based on the learning mechanism which consists of varying the parameters of the parameterized functions (called neurons) of the neural network in order to minimize a criterion previously named cost function. This criterion is usually presented by the mean squared error.

RESULTS AND DISCUSSION

Rainfall regionalization

The first PCA axis accounts for 61.55% of the total data variability (Figure 3). With the second axis, they reflect 86.2% of the precipitation data variability. Therefore, the residual variability that is described by the remaining axes is rather weak and will thus not be considered in the following discussions.

Dimension 1 opposes Aghbalou and Sidi Hssaine stations (strongly positive coordinate on the axis) to the group of stations of Talmest, Adamna, Igrounzar and the group of Chichaoua, Takerkoust, Abadla, and Marrakesh (strongly negative coordinate on the axis). The group containing the stations of Aghbalou and Sidi Hssain is
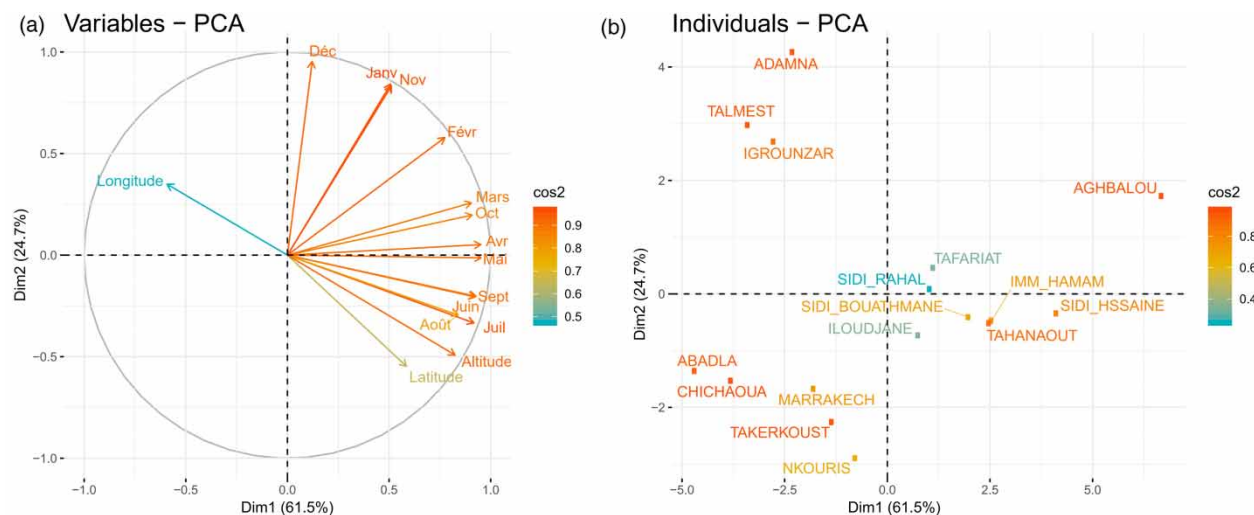
Figure 3 │ Principal component analysis of variables and station-based rainfall time series (individuals).

distinguished by high elevations as well as other variables such as high rainfall amount from February to October. The station of Aghbalou is the main representative of dimension 1 (Figure 4(a)). The second group composed of the stations Talmest, Adamna, and Igrounzar is characterized by relatively lower values of elevation, latitude, less rainfall amounts from June to September, and high rainfall amounts in December. The third group, composed of the stations Chichaoua, Takerkoust, Abadla, and Marrakech, shares relatively lower rainfall values from October to April.

Axis 2 opposes individuals such as the stations Talmest, Adamna, and Igrounzar, which are characterized by high values of rainfall in December, to individuals like the stations Chichaoua, Takerkoust, Abadla, and Marrakech, which receive less rainfall during this month. The variable

'December' is, moreover, extremely correlated with this dimension and it therefore largely represents dimension 2 (Figure 4(b)).

The global classification reveals three main classes (Figure 5):

Class 1 is composed of coastal stations with an oceanic climate: Adamna, Igrounzar, and Talmest. This group is characterized by a certain regularity of rainfall in autumn and winter and by a very pronounced drought in summer.

Class 2 is composed of inland plain stations: Abadla, Chichaoua, Marrakech, and Takerkoust. This group is characterized by low rainfall throughout the year. The station of Nkouris is within this group despite its high altitude because it is under the influence of the 'shelter effect'.
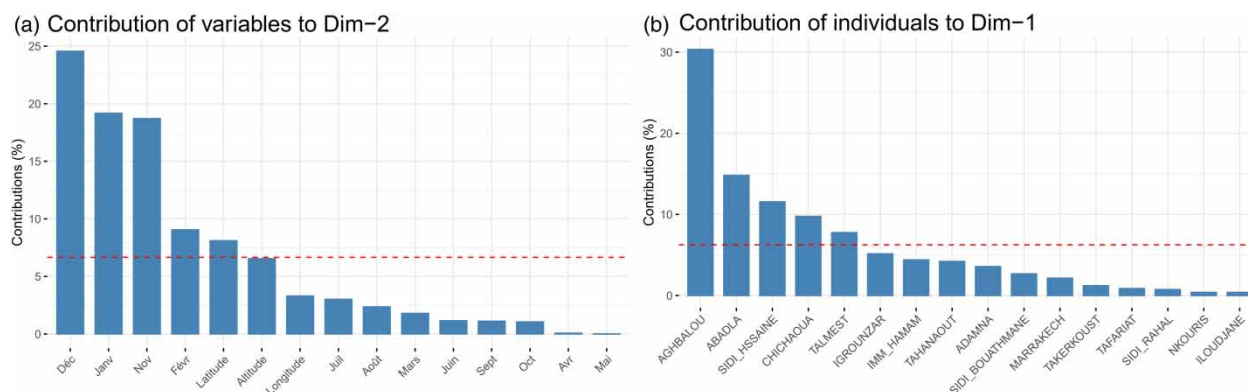

Figure 4 │ Contribution of individuals (a) and variables (b) in the PCA dimensions.
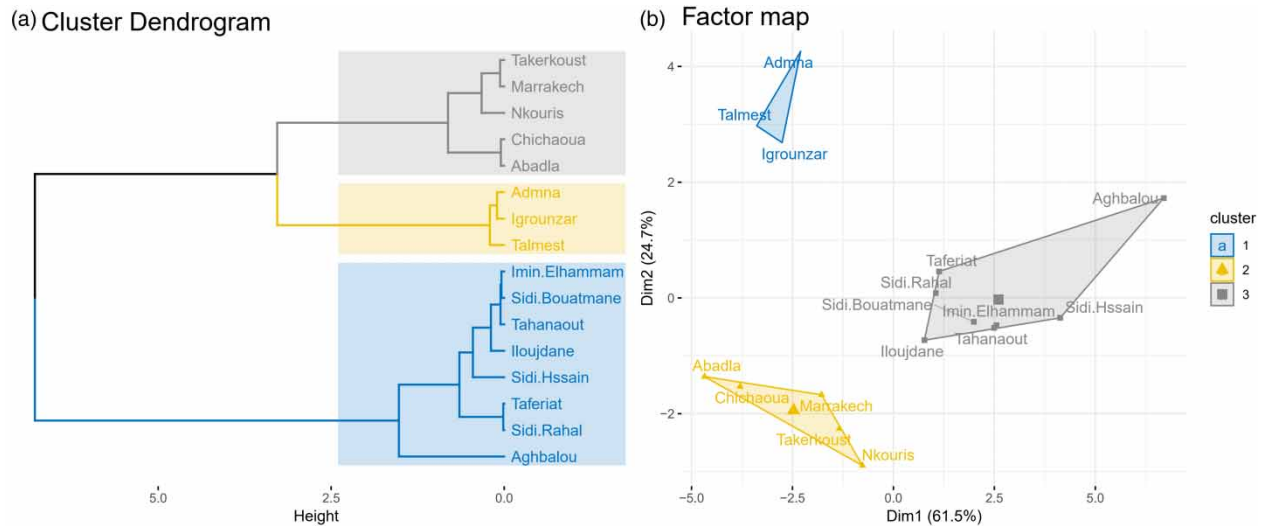
Figure 5 │ Classification and ascending hierarchy of meteorological stations where rainfall data have been retrieved for this study.

This site has always been an exception in the rainfall of Tensift basin, because of its location at the bottom of a valley, and it does not faithfully illustrate the overall rainfall of its region.

Class 3 is composed of mountain stations such as Aghbalou and Sidi Hssain, as well as Tahanaout, Imin El Hammam, Sidi Rahal, Taferiate, Sidi Bouatmane, and Illoujdane. This group stands out (compared to the other two classes) by higher spring (Mar–Apr–May) and summer rainfall amounts. The mountainous climate here favors significant rainfall during the months of March and April, as well as convective and stormy showers during the summer.

Climate change and rainfall trends using the standardized precipitation index (SPI)

In Morocco, drought has always been reported by historians, but its frequency and intensity seems to have increased in the last decades. Several authors have noted significant decreases in precipitation and increases in temperature (Schilling *et al.* 2012; Tramblay *et al.* 2013; Seif-Ennasr *et al.* 2016; Ait Brahim *et al.* 2017; Fniguire *et al.* 2017; Filahi *et al.* 2017; Bouras *et al.* 2019). Indeed, the climate evolution in the 20th century shows that the Mediterranean region has undergone a warming of almost 2 °C. This warming is greater than the global average which is around 0.7 to

0.8 °C. By 2100, specialists predict a warming of 2.5 to 4.5 °C for the Maghreb countries compared to temperatures recorded at the end of the 20th century (IPCC 2008).

In order to detect potential rainfall deficit, we will analyze rainfall evolution over 47 years and show its trends. For this purpose, we will analyze the temporal rainfall variability and compute the standardized precipitation index (SPI); this, for each homogeneous rainfall class (Figure 6). The SPI is an index developed by McKee *et al.* (1993). It is given by the difference of the precipitation from the mean, then dividing it by the standard deviation:

$$\text{SPI} = \frac{(P_i - P_m)}{\sigma}$$

where P_i is precipitation of year i; P_m is average precipitation of the whole study period; and σ is standard deviation.

Drought is noted when this index begins to be negative. Negative SPI values therefore represent a precipitation deficit while positive values indicate that precipitation has been above the historical average. Several authors have defined SPI value ranges to identify the climate aridity or humidity. The one proposed by Lloyd-Hughes & Saunders (2002) is as in Table 2.

The annual precipitation amounts vary widely from year to year. But overall, during the 47 years of data, there is a downward trend in the mid-mountain area (Aghbalou) and in the plain (Marrakech). However, for the coastal station
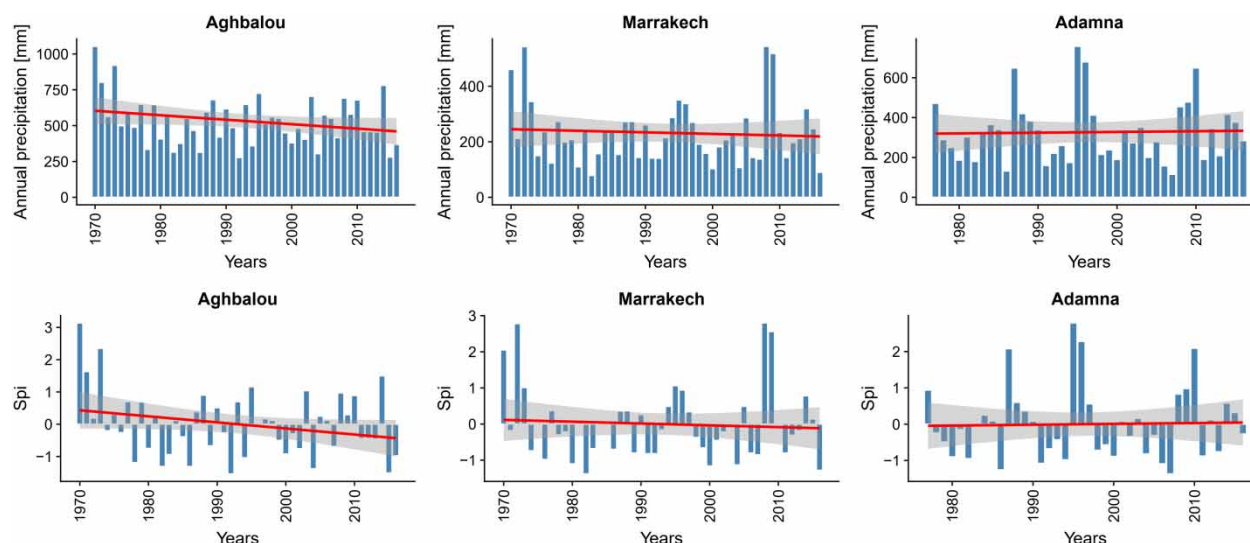
Figure 6 | Trends in annual precipitation and SPI of Aghbalou, Marrakech, and Adamna stations.

Table 2 | Drought classification by SPI value (Lloyd-Hughes & Saunders 2002)

SPI value	Category
2.00 or more	Extremely wet
1.50 to 1.99	Severely wet
1.00 to 1.49	Moderately wet
0 to 0.99	Mildly wet
0 to −0.99	Mild drought
−1.00 to −1.49	Moderate drought
−1.50 to −1.99	Severe drought
−2 or less	Extreme drought

(Adamna), whose data begins in 1977, there is no significant decrease in these precipitation amounts. The SPI obviously confirms the downward trend of the first two stations which is more pronounced in Aghbalou. Historically, the Moroccan mountain has therefore recorded the most rainfall deficit, compared to the normal, in contrast to the coastal zone.

The figure shows more negative SPI values. These values certainly show moderate drought but the dry years are more numerous. They often follow one or two very wet years. The dry sequences are therefore longer than the wet ones. They signal potential water shortages.

Otherwise, future changes in precipitation in the Tensift region, using the RCP4.5 and RCP8.5 scenarios for the horizons 2065 and 2095, have been evaluated by a few authors

(Driouech et al. 2010; Filahi et al. 2017; Marchane et al. 2017). According to the climatic data of the Marrakech region, they all deduced a probable decrease in precipitations which is particularly pronounced in winter and in spring. The expected changes are −22% in the RCP4.5 scenario and −31% for the RCP8.5 scenario. Furthermore, for heavy precipitation events, there are high uncertainties in the projections and the simulation models disagree about future changes (Filahi et al. 2017).

Frequency analysis and variability of rainfall extremes

Adjustment of Weibull, Log normal, Loglogistic, GEV and Gumbel laws to the maximum daily rainfall in the Tensift watershed (Figure 7) made it possible to judge their suitability for this arid to semi-arid environment. The AIC and BIC criteria show that eight stations (Abadla, Adamna, Chichaoua, Imin El hammam, Marrakech, Sidi Hssain, Talmest, and Taferiat) are better adapted to the Log normal law, whereas three stations (Igrounzar, Tahanaout, and Takerkoust) are rather adapted to the GEV law, two stations (Sidi Bouatmane and Nkouris) seem to be better represented by the Gumbel law, and two others (Aghbalou and Illoujdane) by Weibul and only one station (Sidi rahal) adapts better to log-logistic law (Table 3).

The Log normal distribution, therefore, seems to be the suitable probability distribution for modeling maximum
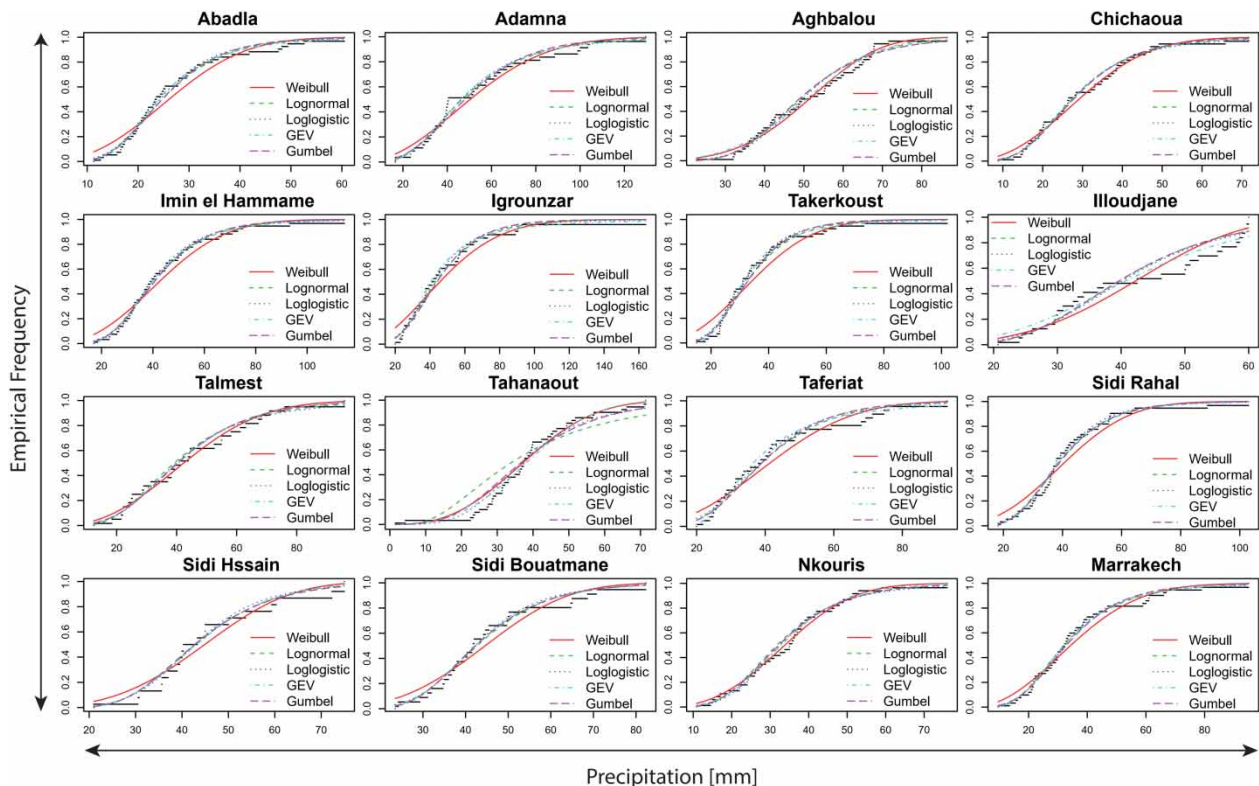
Figure 7 │ Adjustment of statistical distributions to maximum daily rainfall from 1970–1971 to 2016–2017.

daily precipitation, as has been verified elsewhere in the Mediterranean region by the aforementioned studies. Application of this law to estimate daily quantiles (Table 4) has shown that certain areas of the basin can experience very high daily values of precipitation. The first class, previously indicated by the PCA, composed of the coastal stations of Adamna, Igrounzar, and Talmest, stands out from the crowd by very high forecasts of 50-year and 100-year daily rainfall. These estimates all exceed 100 mm per day. They even reach up to 182 mm for the 100-year daily rainfall in Igrounzar. Such rainfall amounts call for particular vigilance in these coastal areas, especially in the city of Essaouira which is surrounded by these three stations. This coastal city has experienced an increasing trend of intense rainfall in recent years (Choukrani et al. 2018). Social adaptation to large amounts of rainfall concentrated in a short time is highly required for rational management of urban hydrology. The forecast for Marrakech city is relatively high with 100-year rainfall of about 97 mm per day. The same

observation is made for some mountain stations, notably Imin El Hammam and Taferiate (Figure 8). However, in the interior plain, Chichaoua and Abadla stations, assembled by the PCA in a low-rainfall region, are also distinguished here by relatively weak quantiles, even for quite large return periods (Figure 8).

That excessive rainfall in these Mediterranean and oceanic areas evokes the debate over climatic upheavals, because, although the increase in temperatures has been proposed in many places around the the world, thus confirming the reality of global warming (Christensen et al. 2007), and the precipitation trend is more nuanced. While the overall forecast for the Mediterranean area tends towards a decrease of the annual rainfall amount, certain exceptions have been noted, particularly for coastal areas of the Maghreb (Nouaceur et al. 2013).

Furthermore, during the month of November 2014, unusual atmospheric conditions were observed along the Moroccan Atlantic coastline. The westerly winds jet-stream, which usually flows from west to east around

Table 3 | Criteria for evaluating frequency models for maximum daily rainfall

Stations	Criteria	Weibull	Lognormal	Loglogistic	GEV	Gumbel
Abadla	AIC	358.22	**347.19**	348.01	347.92	347.60
	BIC	361.92	**350.89**	351.71	353.47	351.30
Admna	AIC	373.79	**369.10**	370.85	371.63	370.75
	BIC	377.17	**372.48**	374.22	376.69	374.13
Aghbalou	AIC	**382.45**	382.97	385.39	384.72	384.22
	BIC	**386.15**	386.67	389.09	390.27	387.92
Chichaoua	AIC	368.02	**363.81**	365.69	366.15	364.25
	BIC	371.68	**367.47**	369.35	371.63	367.91
Imin El Hammam	AIC	408.89	**397.58**	397.93	398.91	398.19
	BIC	412.60	**401.28**	401.63	404.46	401.89
Igrounzar	AIC	342.63	330.25	330.74	**329.34**	333.19
	BIC	345.85	333.47	333.96	**334.17**	336.41
Takerkoust	AIC	390.39	373.44	372.71	**371.61**	373.91
	BIC	394.09	377.14	376.41	**377.16**	377. 61
Illoujdane	AIC	**226.62**	227.80	230.71	232.10	228.30
	BIC	**229.29**	230.46	233.37	236.09	230.97
Talmest	AIC	265. 37	**265.23**	266.88	267.25	265.27
	BIC	268.17	**268.03**	269.68	271.45	268.07
Tahanaout	AIC	384.62	417.08	392.99	**381.52**	387.53
	BIC	388.28	420.73	396.64	**387.01**	391.18
Taferiat	AIC	285.91	**278.79**	280.65	278.74	279.81
	BIC	288.91	**281.78**	283.64	283.23	282.80
Sidi Rahal	AIC	395.30	382.14	**380.83**	383.45	381.96
	BIC	399.00	385.84	**384.53**	389.00	385.66
Sidi Hssain	AIC	157.42	**155.31**	155.33	157.18	155.34
	BIC	159.31	**157.20**	157.22	160.01	157.23
Sidi Bouatmane	AIC	232.02	226.90	227.48	228.68	**226.71**
	BIC	234.68	229.57	230.14	232.68	**229.37**
Nkouris	AIC	338.15	338.49	338.88	338.93	**337.70**
	BIC	341.62	341.96	342.36	344.14	**341.18**
Marrakech	AIC	391.66	**384.94**	385.43	386.95	385.92
	BIC	395.31	**388.60**	389.08	392.43	389.57

Bold numbers indicate the lowest values of AIC and BIC criteria and therefore the most appropriate distributions.

latitudes 50–60° north above the Atlantic Ocean, abnormally descended in latitude, especially in the last ten days of the month. The southern branch of this stream caused a flow of sea air to Morocco, and large parts of the west-central areas of the country experienced one of the rainiest months in their modern history. From 20 to 30 November 2014, the three stations of the first group (Adamna, Igrounzar, and Talmest) received cumulative rainfall of 249, 216, and 245 mm, respectively. These rainfall amounts are similar to the annual average of rainfall in Marrakech, for example.

Spatialization of centennial daily rainfall

From measurement points, several interpolation methods allow the spatialization of precipitation over a geographical area (Ly *et al.* 2013). However, it is important to choose the one that best replicates the data (Caruso & Quarta 1998). The number of measuring stations and their dispersion in the watershed are important factors to consider, because in mountainous areas, for example, rainfall amounts are more difficult to predict because of their complex topography (Johnson & Hanson 1995; Buytaert *et al.* 2006).

Table 4 | Estimation of daily rainfall quantiles in the Tensift watershed

ID	Stations	100 Years	50 Years	10 Years	2 Years
S1	Admna	148.5	129.6	88.3	46.7
S2	Igrounzar	182.5	143.5	80.5	40.5
S3	Talmest	119.8	105.1	72.5	39.2
S4	Illoujdane	71.1	67.9	58.7	42.3
S5	Chichaoua	76.5	67.8	48.1	27.3
S6	Abadla	59.4	53.6	40.1	24.8
S7	Sidi_Bouatmane	88.5	80.9	62.9	42.3
S8	Sidi_Hssain	86.7	79.9	63.2	42.9
S9	Takerkoust	95.9	81.2	53.5	31.4
S10	Nkouris	79.8	71.9	53.4	32.2
S11	Imin_El_Hammam	101.1	90.8	67.0	40.5
S12	Marrakech	96.6	84.9	59.0	32.2
S13	Tahanaout	72.0	68.6	57.7	38.3
S14	Aghbalou	81.2	78.0	68.7	51.4
S15	Taferiat	98.6	88.4	64.9	38.8
S16	Sidi_Rahal	92.6	81.0	58.5	38.4

In the Tensift watershed, frequency analysis allowed estimation of 100 years of rainfall. To spatialize this precipitation, we used a black box model because of its properties of parsimony and universal approximation (Piron *et al.* 1997). Artificial neural networks are an example that can solve problems of identification and prediction (Ruano 2005). Consisting of multiple layers, the network has a learning algorithm and an aptitude for approximation and generalization (Huang 2009). The simplest is composed of three layers: an input layer, one or more hidden layers, and an output layer (Figure 9(a)). Our input data are composed of XYZ coordinates of the rainfall stations and their centennial precipitation. After several tests on different architectures of the model, the one that provided the best Nash criteria to simulate precipitations was chosen. This model has three layers: an input layer with three neurons, a hidden layer of 12 neurons, and a last output layer of a single neuron. To evaluate its performance, we established a linear regression between the observed and the predicted rainfall values of all stations (Figure 9(b)).

The important coefficient of determination R^2 (0.95) illustrates the good correlation between the two groups of values. The ANN model thus reproduces the precipitation amount well and, therefore, it can be used for the spatial representation of precipitation. From a digital elevation model and coordinates of different pixels, a map of 100-year average of daily rainfall is established (Figure 10). The map
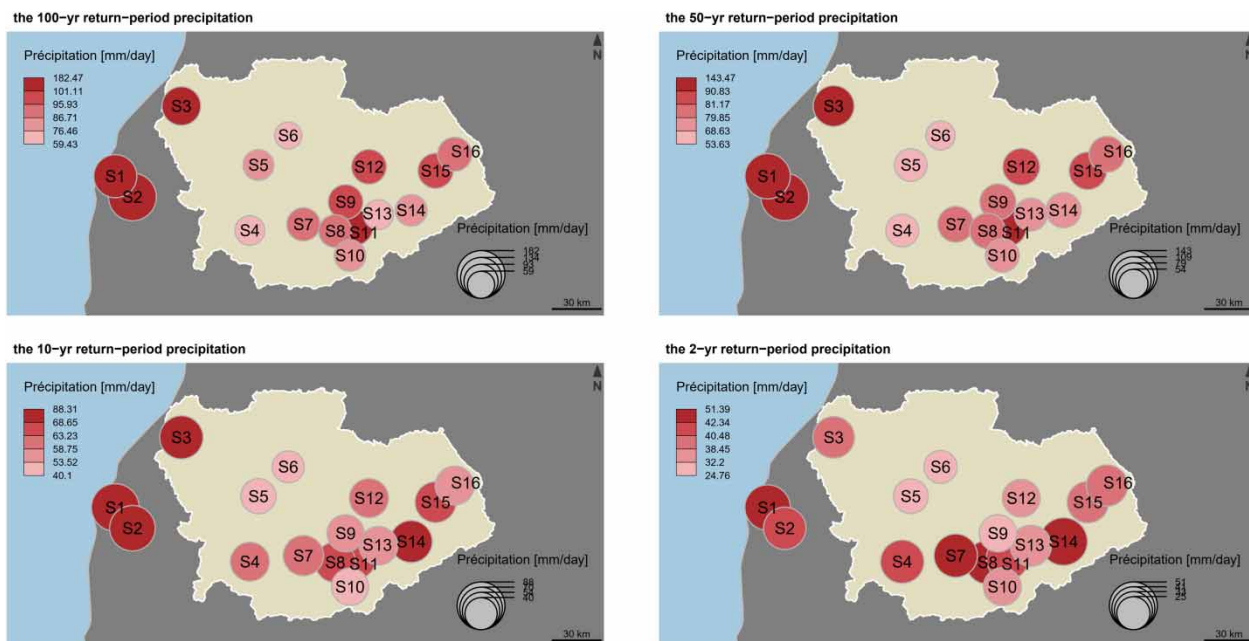
Figure 8 | Amounts and variability of 2-, 10-, 50-, and 100-year return periods of rainfall in the Tensift watershed.
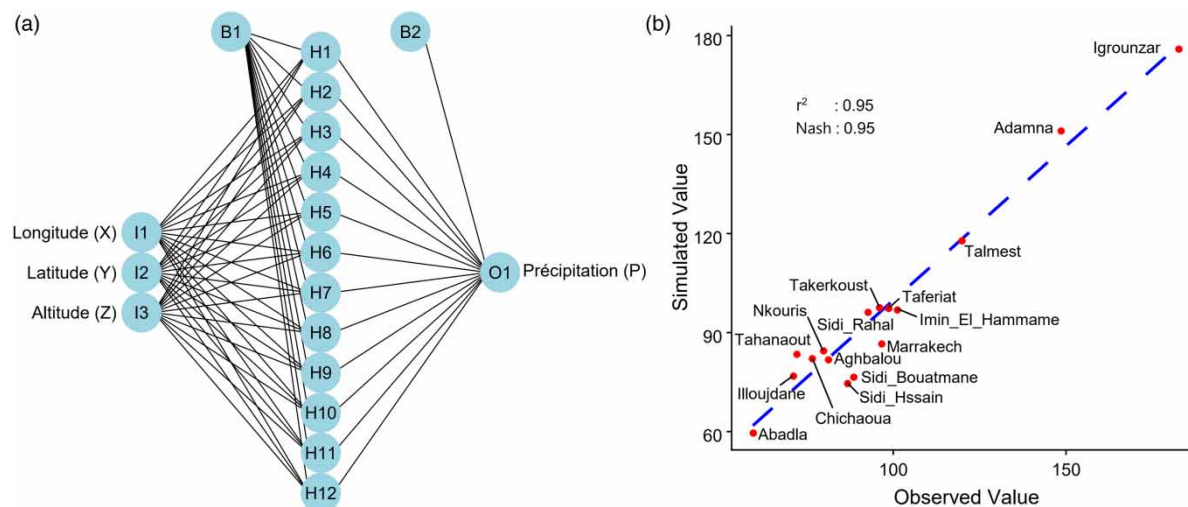
Figure 9 │ (a) Structure of the artificial neural network; (b) correlation between the observed and simulated 100-year daily rainfall using the ANN model.

reveals several areas that seem to be favorable to heavy showers, including the coastal regions and the foothills of the High Atlas Mountains. Extreme rainfall events in these areas have a high ability to generate significant floods in the future, as was the case several times during recent

years (Baiddah et al. 2012; Saidi et al. 2012, 2013; El Alaoui El Fels et al. 2017, 2018; El Khalki et al. 2018).

Model outputs also reveal changes in centennial precipitation, depending on longitude (X), latitude (Y), and altitude (Z) (Figure 11). Like the result of PCA and frequency
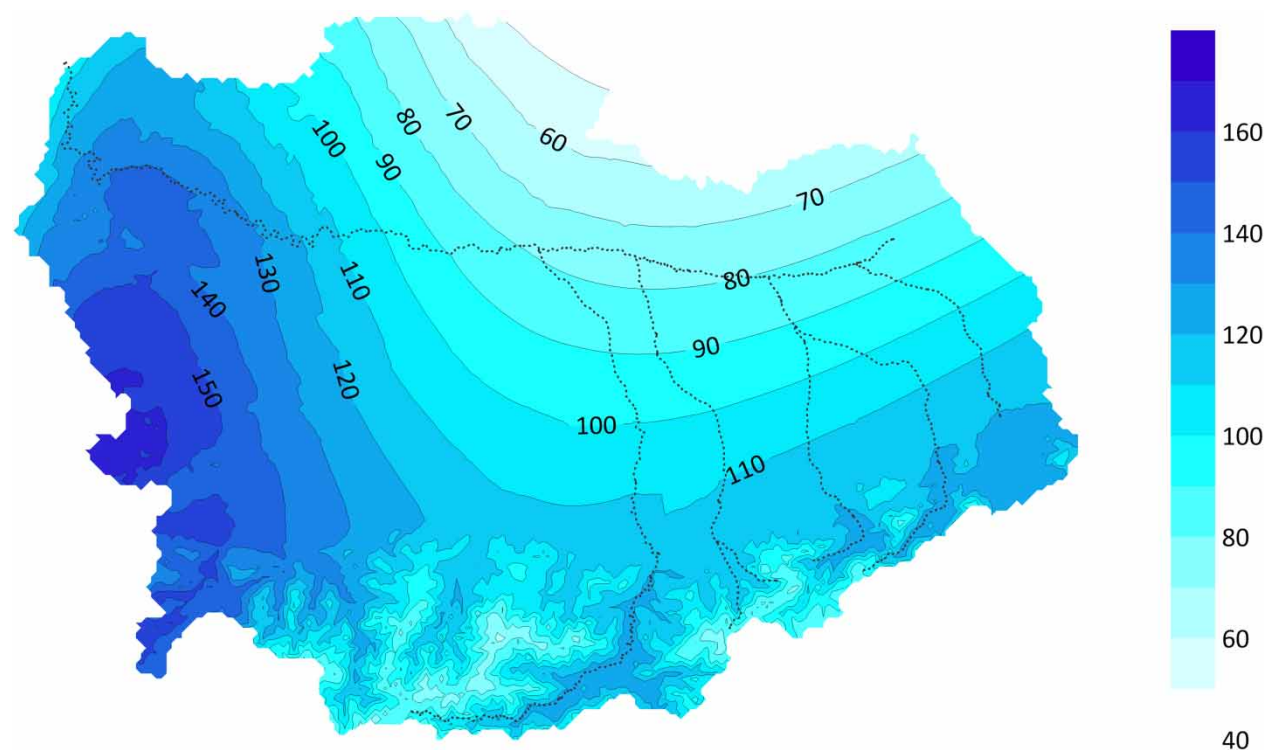

Figure 10 │ Spatial distribution of the 100-year average of daily rainfall over the Tensift watershed in western central Morocco.
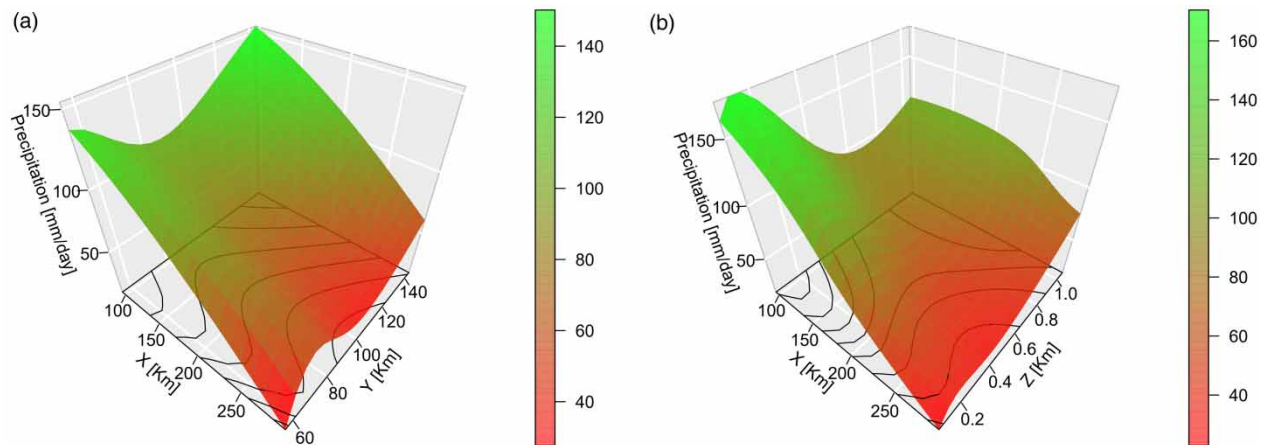
Figure 11 │ Three-dimensional variations of the 100-year average of daily rainfall according to X–Y (a) and X–Z (b) coordinates.

analysis, these centennial quantiles vary greatly by longitude (distance from the ocean) much more than by latitude (in the north–south direction), whereas a slight increase is noted on the High Atlas Mountains and a decrease of precipitation is observed on the plain (Figure 11(a)). The altitude (Z) also impacts on these quantiles, but in a more moderate way than longitude (Figure 11(b)). Indeed, the 100-year average of daily rainfall shows an increase from the plain (example Abadla, Chichaoua) towards the High Atlas Mountains (Imin el Hammam, Taferiate, Sidi Rahal, etc.).

CONCLUSION

The variability and the spatial distribution of rainfall, using ANN, in Tensift in western central Morocco reveals the existence of three homogeneous geographic areas. These areas are distinguished by different rainfall behaviors. The coastal areas stand out by their exposure to important and intense precipitations. More attention should be given to these areas for their high potential of hydrological hazards. For instance, the ten-year daily rainfall (more than 80 mm in Adamna and Igrounzar) exceeds the 100-year daily rainfall in other stations. Contrariwise, the middle of the Tensift plain is characterized by a rainfall deficit, either on daily or annual time scales, and rainfall is not particularly abundant. The vast agricultural fields and irrigated perimeters of this plain meet their water needs from groundwater. This anthropogenic forcing on groundwater will accentuate

problems related to the availability and quality of water. Alternative solutions are needed to limit these problems. Strengthening dam policy and investing more in surface water storage facilities, especially in the High Atlas Mountains, would be necessary to ensure the agricultural development of the region. For the mid-mountains area, without having exceptional centennial rainfall, it still suprisingly receives a significant amount of precipitation considering its pre-Saharan latitude. This part of the Tensift basin ensures a regular supply of water to the plain, hence giving it the name of 'water tower' of the plain of Marrakech. The knowledge of these homogeneous rainfall areas of Tensift would be of economic interest for knowledge of the hydrological contributions of the ungauged sub-basins, and more generally for the management of rainwater as well as for the management of the measuring network. This network will have to be strengthened, especially on the right bank of Tensift Wadi, which is clearly under-equipped and lacks sufficient hydrological monitoring.

Finally, for Morocco and its region, whereas different forecasts and different climate scenarios predict warmer climates with a decrease of annual amount of precipitation by the end of the 21st century, there might be an exception in the coastal areas, where more extreme rainfall events took place during the last decades. The high amounts are mainly explained by rainfall intensification over short time periods. Annual rainfall is indeed associated with more marked extremes. These therefore announce potential hydrological hazards in the region.

REFERENCES

Ait Brahim, Y., Saidi, M. E., Kouraiss, K., Sifeddine, A. & Bouchaou, L. 2017 Analysis of observed climate trends and high resolution scenarios for the 21st century in Morocco. *Journal of Materials and Environmental Sciences* **8** (4), 1375–1384.

Akaike, H. 1974 A new look at statistical model identification. *IEEE Transactions on Automatic Control* **19**, 716–722.

Baiddah, A., Saidi, M. E., Daoudi, L., El Mimouni, A. & Smaij, Z. 2012 Typologie des crues en zone montagneuse, océanique et semi-aride. Le cas du bassin versant du Ksob (Haut Atlas occidental, Maroc). (Floods typology in mountainous, oceanic and semiarid area. Case of the Ksob watershed (Western High Atlas, Morocco)). *Larhyss Journal* **11**, 79–96.

Benson, M. A. 1968 Uniform flood frequency estimation methods for federal agencies. *Water Resources Research* **4** (5), 891–908.

Bouras, E., Jarlan, L., Khabba, S., Er-Raki, S., Dezetter, A., Sghir, F. & Tramblay, Y. 2019 Assessing the impact of global climate changes on irrigated wheat yields and water requirements in a semi-arid environment of Morocco. *Scientific Reports* **9**, 19142. https://doi.org/10.1038/s41598-019-55251-2.

Buytaert, W., Célleri, R., Willems, P., De Bièvre, B. & Wyseure, G. 2006 Spatial and temporal rainfall variability in mountainous areas: a case study from the South Ecuadorian Andes. *Journal of Hydrology* **329** (3–4), 413–421. doi:10.1016/j.jhydrol.2006.02.031.

Cai, K., Zhang, M., Yu, Y. & Kim, K. 2019 Pollution, source, and relationship of trace metal(loid)s in soil-wheat system in Hebei Plain, Northern China. *Agronomy* **9**, 391.

Caruso, C. & Quarta, F. 1998 Interpolation methods comparison. *Computer and Mathematics with Applications* **35** (12), 109–126.

Chaouche, K., Hubert, P. & Lang, G. 2002 Graphical characterisation of probability distribution tails. *Stochastic Environmental Research and Risk Assessment* **16** (5), 342–357.

Choukrani, G., Hamimsa, A., Saidi, M. E. & Babqiqi, A. 2018 Diagnosis and future projection of climate change in arid zone. Case of Marrakech-Safi region (Morocco). *Larhyss Journal* **36**, 49–63.

Christensen, J. J., Hewitson, B., Busuioc, A., Chen, A., Gao, X., Held, I., Jones, R., Kollie, R. K., Kwon, W. T., Laprise, R., Magana Rueda, V., Mearns, L., Menendez, C. G., Raisanen, J., Rinke, A., Sarr, A. & Whetton, P. 2007 *Regional Climate Projections. In*: Climate Change (2007): The Physical Science Basis. Contribution of Working Group 1 to the Fourth Assessment Report of the Intergovernmental Panel on Climate Change. Cambridge University Press, Cambridge, UK and New York, NY, USA, pp. 847–940.

Ding, Z., Lu, R. & Wang, Y. 2019 Spatiotemporal variations in extreme precipitation and their potential driving factors in non-monsoon regions of China during 1961–2017.

Environmental Research Letters **14**, 024005. https://doi.org/10.1088/1748-9326/aaf2ec.

Driouech, F., Déqué, M. & Sánchez-Gómez, E. 2010 Weather regimes-Moroccan precipitation link in a regional climate change simulation. *Global Planetary Change* **72**, 1–10.

El Alaoui EL Fels, A., Alaa, N. & Bachnou, A. 2017 Combination of GIS and mathematical modeling to predict floods in semiarid areas: case of Rheraya watershed (Western High Atlas, Morocco). *Arabian Journal of Geosciences* **10**, 554. doi:10.1007/s12517-017-3345-x.

El Alaoui EL Fels, A., Alaa, N., Bachnou, A. & Rachidi, S. 2018 Flood frequency analysis and generation of flood hazard indicator maps in a semi-arid environment, case of Ourika watershed (western High Atlas, Morocco). *Journal of African Earth Sciences* **141**, 94–106. doi:10.1016/j.jafrearsci.2018.02.004.

El Khalki, E., Tramblay, Y., Saidi, M. E., Bouvier, C., Hanich, L., Benrhanem, M. & Alaouri, M. 2018 Comparison of modeling approaches for flood forecasting in the High Atlas Mountains of Morocco. *Arabian Journal of Geosciences* **11**, 410. doi:10.1007/s12517-018-3752-7.

Ferrer, J. P. 1992 Analyse statistique de pluies maximales journalières Comparaison de différentes méthodes et application au bassin Guadalhorce (Espagne). (Statistical analysis of maximum daily rainfall. Comparison of different methods and application in the Guadalhorce basin (Spain)). *Hydrologie Continentale* **7** (1), 23–31.

Filahi, S., Tramblay, Y., Mouhir, L. & Diaconescu, E. P. 2017 Projected changes in temperature and precipitation in Morocco from high-resolution regional climate models. *International Journal of Climatology* **37** (14), 4846–4863. http://dx.doi.org/10.1002/joc.5127.

Fisher, R. A. 1922 On the mathematical foundations of theoretical statistics. *Philosophical Transactions of the Royal Society A* **222A**, 309–368.

Fniguire, F., Laftouhi, N. E., Saidi, M. E., Zamrane, Z., El Himer, H. & Khalil, N. 2017 Spatial and temporal analysis of the drought vulnerability and risks over eight decades in a semi-arid region (Tensift basin: Morocco). *Theoretical and Applied Climatology* **130**, 321–330. doi:10.1007/s00704-016-1873-z.

Goula, A. B. T., Soro, E. G., Kouassi, W. & Srohourou, B. 2012 Tendances et ruptures au niveau des pluies journalières extrêmes en Côte d'Ivoire (Afrique de l'Ouest). (Trends and shifts in extreme daily rainfall in Ivory Coast (West Africa)). *Journal des Sciences Hydrologiques* **57** (6), 1067–1080.

Greenwood, J. A., Landwerh, J. M., Matalas, N. C. & Wallis, J. R. 1979 Probability weighted moments: definition and relation to parameters of several distributions express able in inverse form. *Water Resources Research* **15**, 1049–1054.

Habibi, B., Meddi, M. & Boucefiane, A. 2012 Analyse fréquentielle des pluies journalières maximales Cas du Bassin Chott-Chergui. (Frequency analysis of maximum daily rainfall. Case of the Chott-Chergui Basin). *Nature & Technologie, Sciences de l'Environnement* **8**, 41–48.

Härdle, W. K. & Simar, L. 2012 Canonical correlation analysis. In: *Applied Multivariate Statistical Analysis* (W. K. Härdle & L. Simar, eds). Springer, Berlin, Heidelberg. https://doi.org/10.1007/978-3-642-17229-8_15.

Hiez, G. 1977 Homogénéisation des données pluviométriques. (Homogenization of rainfall data). *Cahiers ORSTOM, série Hydrologie* **XIX** (2), 129–172.

Hosking, J. R. M. 1990 L-moments: analysis and estimation of distributions using linear combinations of order statistics. *Journal of the Royal Statistical Society Series B* **52**, 105–124.

Huang, Y. 2009 Advances in artificial neural networks-methodological development and application. *Algorithms* **2** (3), 973–1007.

IEA (Institution of Engineers, Australia) 1977 *Australia Rainfall and Runoff: Flood Analysis and Design*. IEA, Canberra, Australia.

Intergovernmental Panel on Climate Change (IPCC) 2008 *2007 Balance Sheet of Climate Change: Assessment Report Synthesis of the Intergovernmental Panel on Climate Change (IPCC)*. World Meteorological Organization (WMO)/United Nations Environment Program (UNEP). Geneva, Switzerland, 103 p.

Johnson, G. L. & Hanson, C. L. 1995 Topographic and atmospheric influences on precipitation variability over a mountainous watershed. *Journal of Applied Meteorology* **34** (1), 68–87.

Kidson, R. L. & Richards, K. S. 2005 Flood frequency analysis: assumptions and alternatives. *Progress in Physical Geography* **29** (3), 392–410.

Kim, S. M., Kang, M. S. & Jang, M. W. 2018 Assessment of agricultural drought vulnerability to climate change at a municipal level in South Korea. *Paddy and Water Environment* **16**, 699. https://doi.org/10.1007/s10333-018-0661-z.

Koutsoyiannis, D. 2004 Statistics of extremes and estimation of extreme rainfall: I. Theoretical investigation. Hydrological Sciences **49** (4), 575–590.

Kritsky, S. N. & Menkel, F. M. 1969 On principles of estimation methods of maximum discharge. *IAHS Publ* **84**, 53–63.

Lancelot, R. & Lesnoff, M. 2005 Sélection *de modèles avec l'AIC et critères d'information dérivés. (Selection of models with AIC and derived information criteria)*. CIRAD Publications, Montpellier, France, 7 p.

Li, X., Zhang, X., Zhang, P. & Zhu, G. 2019 Fault data detection of traffic detector based on wavelet packet in the residual subspace associated with PCA. *Applied Sciences* **9**, 3491. doi:10.3390/app9173491.

Lloyd-Hughes, B. & Saunders, M. A. 2002 A drought climatology for Europe. *International Journal of Climatology* **22**, 1571–1592. https://doi.org/10.1002/joc.846.

Ly, S., Charles, C. & Degré, A. 2013 Different methods for spatial interpolation of rainfall data for operational hydrology and hydrological modeling at watershed scale. A review. *Biotechnolology, Agronomy, Society and Environment* **17** (2), 392–406.

Malmgren, B. A. & Winter, A. 1999 Climate zonation in Puerto Rico based on principal components analysis and an artificial neural network. *Journal of Climate* **12**, 977–985. doi:10.1175/1520-0442(1999)012<0977:CZIPRB>2.0.CO;2.

Marchane, A., Tramblay, Y., Hanich, L., Ruelland, D. & Jarlan, L. 2017 Climate change impacts on surface water resources in the Rheraya catchment (High-Atlas, Morocco). *Hydrological Sciences Journal* **62** (6), 979–995. http://dx.doi.org/10.1080/02626667.2017.1283042.

McCulloch, W. S. & Pitts, W. 1943 A logical calculus of the ideas immanent in nervous activity. *Bulletin of Mathematical Biophysics* **5**, 115–133. http://dx.doi.org/10.1007/BF02478259.

McKee, T. B., Doesken, N. J. & Kleist, J. 1993 The relationship of drought frequency and duration of time scales. In: *Eighth Conference on Applied Climatology*, January 17–23, 1993, Anaheim, CA, USA. American Meteorological Society, pp. 179–186.

Merzougui, A. & Slimani, M. 2012 Régionalisation des lois de distribution des pluies mensuelles en Tunisie. (Regionalization of statistical distributions fitted to monthly rainfall in Tunisia). *Hydrological Sciences Journal* **57** (4), 668–685. doi:10.1080/02626667.2012.670702.

NERC Natural Environment Research Council 1975 *Flood Studies Report, Vol. 1 (Hydrological Studies) and Vol. 2 (Meteorological Studies)*, Institute of Hydrology, Wallingford, UK.

New, M., Todd, M., Hulme, M. & Jones, P. 2001 Precipitation measurements and trends in the twentieth century. *International Journal of Climatology* **21**, 1899–1922. doi:10.1002/joc.680.

Nouaceur, Z., Laignel, B. & Turki, I. 2013 Changements climatiques au Maghreb: vers des conditions plus humides et plus chaudes sur le littoral algérien? (Climate change in the Maghreb: towards wetter and warmer conditions on the Algerian coast?). *Physio-Géo* **7-1**, 307–323. doi:10.4000/physio-geo.3686.

Onibon, H., Ouarda, T., Barbet, M., St-Hilaire, A., Bobee, B. & Bruneau, P. 2004 Analyse fréquentielle régionale des précipitations journalières maximales annuelles au Québec, Canada. (Regional frequency analysis of annual maximum daily precipitation in Quebec, Canada). *Hydrological Sciences Journal* **49** (4), 717–735.

Papalexiou, S. M. & Koutsoyiannis, D. 2006 A probabilistic approach to the concept of Probable Maximum Precipitation. *Advances in Geosciences, European Geosciences Union* **7**, 51–54.

Piron, E., Latrille, E. & René, F. 1997 Application of artificial neural networks for crossflow microfiltration modelling: 'black-box' and semi-physical approaches. *Computers & Chemical Engineering* **21** (9), 1021–1030. https://doi.org/10.1016/S0098-1354(96)00332-8.

Planton, S., Deque, M., Douville, H. & Spagnoli, B. 2005 Impact du réchauffement climatique sur le cycle hydrologique. (Impact of global warming on the hydrological cycle). *Comptes Rendus Geoscience* **337**, 193–202. doi:10.1016/j.crte.2004.10.003.

Rao, R. A. & Hamed, K. H. 2000 *Flood Frequency Analysis*. CRC Press, Boca Raton, FL, USA, 350 p.

Raqab, M. Z., Bdair, O. M., Madi, M. T. & Alqallaf, F. A. 2018 Prediction of the remaining testing time for the generalized Pareto progressive censoring samples with applications to extreme hydrology events. *Journal of Statistical Theory and Practice* **12** (2), 165–187. doi:10.1080/15598608.2017.1338168.

Ringnér, M. 2008 What is principal component analysis? *Nature Biotechnology* **26**, 303–304. doi:10.1038/nbt0308-303.

Rossi, F., Fiorentino, M. & Versace, P. 1984 Two component extreme value distribution for flood frequency analysis. *Water Resources Research* **20** (7), 847–856.

Ruano, A. 2005 *Intelligent Control Systems Using Computational Intelligence Techniques*. IEE Publishers, London, UK, 454 p.

Saidi, M. E. M., Boukrim, S., Fniguire, F. & Ramromi, A. 2012 Les écoulements superficiels sur le Haut Atlas de Marrakech. Cas des débits extrêmes. (Superficial flows on the High Atlas of Marrakech. Case of extreme flows). *Larhyss Journal* **10**, 75–90.

Saidi, M. E., Bouloumou, Y., Ed-Daoudi, S. & Aresmouk, M. E. 2013 Les crues de l'oued Issil en amont de Marrakech (Maroc), un risque naturel récurrent. (The floods of Issil wadi upstream of Marrakesh (Morocco), a recurring natural hazard). *European Scientific Journal* **9** (23), 189–208.

Schilling, J., Freier, K. P., Hertig, E. & Scheffran, J. 2012 Climate change, vulnerability and adaptation in North Africa with focus on Morocco. *Agriculture, Ecosystems & Environment* **156**, 12–26. https://doi.org/10.1016/j.agee.2012.04.021

Schwarz, G. 1978 Estimating the dimension of a model. *Annals of Statistics* **6** (2), 461–464.

Seif-Ennasr, M., Zaaboul, R., Hirich, A., NilsCaroletti, G., Bouchaou, L., El Morjani, Z. E., Beraaouz, E., McDonnell, R. A. & Choukr-Allah, R. 2016 Climate change and adaptive water management measures in Chtouka Aït Baha region (Morocco). *Science of the Total Environment* **573**, 862–875. https://doi.org/10.1016/j.scitotenv.2016.08.170.

Shao, Q., Wong, H., Xia, J. & Ip, W. C. 2004 Models for extremes using the extended three-parameter Burr XII system with application to flood frequency analysis. *Hydrological Sciences Journal* **49** (4), 685–702. doi:10.1623/hysj.49.4.685.54425.

Smith, G. L. 1991 Principal components analysis: an introduction. *Analytical Proceedings* **28**, 150–161.

Solomon, S., Qin, D., Manning, M., Chen, Z., Marquis, M., Averyt, K. B., Tignor, M. & Miller, H. L. 2007 Regional Climate Projections. Climate Change 2007: The Physical Science Basis. Contribution of Working Group I to the Fourth Assessment Report of the Intergovernmental Panel on Climate Change, Cambridge University Press, Cambridge, 847–940.

Son, P. N., Vu, C. D. & Anh, M. Q. 2017 Development of a PC program for multivariate statistical analysis. *Communications in Physics* **27** (4), 291–300. doi:10.15625/0868-3166/27/4/10499.

Tramblay, Y., El Adlouni, S. & Servat, E. 2013 Trends and variability in extreme precipitation indices over Maghreb countries. *Natural Hazards and Earth System Sciences* **13**, 3235–3248. https://doi.org/10.5194/nhess-13-3235-2013.

Wania, O., Scheidegger, A., Carbajal, J. P., Rieckermann, J. & Blumensaat, F. 2017 Parameter estimation of hydrologic models using a likelihood function for censored and binary observations. *Water Research* **121**, 290–301. doi:10.1016/j.watres.2017.05.038.

Whitford, W. G. 2002 *Ecology of Desert Systems*, Academic Press, New York. 326 p.

Wilks, D. S. & Cember, R. P. 1993 *Atlas of precipitation extremes for the northeastern United States and southeastern Canada*. NRCC Research Publication RR *93–95*. 40 p.